Diffusion-tensor magnetic resonance imaging of the human heart in health and in acute myocardial infarction using diffusion-weighted echo-planar imaging technique with spin-echo signals

Weronika Mazur[1], Małgorzata Urbańczyk-Zawadzka[2], Łukasz Czyż[3], Ewa Kwiecień[3], Robert Banyś[4], Piotr Musiałek[3], Artur T. Krzyżak[5]

[1]Faculty of Physics and Applied Computer Science, AGH University of Science and Technology, Krakow, Poland

[2]Department of Radiology, John Paul II Hospital, Krakow, Poland

[3]Department of Cardiac and Vascular Diseases, Jagiellonian University, John Paul II Hospital, Krakow, Poland

[4]Department of Radiology, John Paul II Hospital, Krakow, Poland

[5]Faculty of Geology, Geophysics and Environmental Protection, AGH University of Science and Technology, Krakow, Poland

A b s t r a c t

Introduction: Originally thought unsuitable due to proneness to myocardial motion and susceptibility artefacts, spin-echo echo planar imaging (SE-EPI) has gained attention for the cardiac diffusion-weighted imaging (DWI) and diffusion tensor imaging (DTI) offering higher SNR and lower achievable echo time (TE).

Aim: The application of DTI for patients with acute myocardial infarction (AMI) using our methodology developed on the basis of the SE-EPI sequence.

Material and methods: Twelve patients with AMI and six healthy controls were enrolled in the preliminary DTI study within the CIRCULATE STRATEGMED 2 project. Our method relied on a pilot ECG-triggered DTI examination, based on which the initial evaluation was possible and allowed proper manipulation of TE (64/47 ms for patients/control), repetition time (TR) and ECG trigger delay in the consecutive DTI.

Results: The study demonstrated that by using our algorithm it was possible to obtain DWI images showing infarct zones identified on T1-weighted images with late gadolinium-enhancement (LGE) with division into subtle and severe damage. Quantitative DTI showed increased mean diffusivity (MD) and decreased fractional anisotropy (FA) in the infarct compared to remote tissue. The application of B-matrix spatial distribution (BSD) calibration allowed the improvement of FA.

Conclusions: Our algorithm is suitable for qualitative assessment of infarction zones with different severity. The analysis of the quantitative DTI showed that despite the lack of motion compensation blocks in the applied SE-EPI sequence, it was possible to approach the diffusion tensor parameter values reported for the myocardium.

Key words: acute myocardial infarction, cardiac diffusion-weighted imaging, cardiac diffusion tensor imaging, spin-echo echo-planar imaging.

S u m m a r y

In the paper, we present the method for diffusion tensor imaging (DTI) of the human heart *in vivo* based on the commonly available spin-echo echo-planar imaging (SE-EPI) sequence. We show the possibility to non-invasively detect infarct zones with different severity corresponding to T1-weighted images with late gadolinium enhancement (LGE). By application of the B-matrix spatial distribution (BSD) calibration method it was possible to quantitatively analyze DTI metrics and approach the values reported for the myocardium.

Corresponding author:
Weronika Mazur MSc, Faculty of Physics and Applied Computer Science, AGH University of Science and Technology, 30 Mickiewicza Av., 30-059 Krakow, Poland, e-mail: Weronika.Mazur@fis.agh.edu.pl

Introduction

Diffusion-weighted magnetic resonance imaging (dMRI) provides unique information on the structure, organization and integrity of tissue without the need for exogenous contrast agents. In clinical medicine dMRI is widely used in static tissue imaging (such as the brain) to diagnose injury not visible with other techniques and thus to guide clinical decision-making. However, dMRI of the heart, in comparison to the brain, has proven to be technically challenging [1]; dMRI images of the heart applicable in routine clinical management have not yet been systematically obtained. One fundamental difference between the heart and the brain is deformation and displacement of the myocardium during the cardiac cycle. Another challenge arises from the significantly shorter transverse relaxation time of the myocardium, T_2 (~40 ms in the myocardium at 3 T, which is approximately half of the brain white matter value). This results in a low signal-to-noise ratio (SNR) and leads to echo time (*TE*) shortening. Besides the short T_2 values, dMRI of the myocardium *in vivo* is also restricted by the main magnetic field inhomogeneity within the thorax, which results in more susceptibility-related distortions in echo planar imaging (EPI) of the heart [2].

Recently developed B-matrix spatial distribution (BSD) in dMRI may enable minimization of systematic errors due to an inhomogeneous gradient field [3]. BSD is a calibration technique which delivers the actual distribution of the B-matrix in space. It has been suggested that taking into account the spatial variability of the B-matrix may improve the accuracy of diffusion tensor imaging (DTI) [3–5]. Recent data indicate that changes in the diffusivity of water in myocardium correlate with areas of risk [2]. Another important advantage of advancing dMRI imaging of the human heart arises from the fact that DWI and DTI can potentially be applied instead of imaging with the application of gadolinium-based contrast agents [6]. Furthermore, DTI description of the diffusion signal may depict changes in the local cardiac myofiber orientation, a fundamental aspect of cardiac function [7].

Aim

The aim of our study was to apply DTI for the human heart *in vivo* using the spin echo-echo planar imaging (SE-EPI) pulse sequence. SE-EPI was possible by manipulating essential acquisition parameters, including *TE*, repetition time (*TR*) and ECG trigger delay. Furthermore, BSD calibration was performed using in-house developed software that was used for image analysis. Then, pilot evaluation of the applicability of the method developed to obtain dMRI myocardial images was performed in a series of healthy volunteers and patients with acute myocardial infarction (AMI). The method and patients' condition were additionally evaluated based on the follow-up examination.

Material and methods

Model of the heart

The orientation of the heart obeys specific semantics, where three planes are defined: the short axis view, the 2-chamber and the 4-chamber views (also called vertical and horizontal long axis views, respectively). The heart can be divided into three sections along its long axis – basal, mid and apical cavity. In the short axis view, the left ventricle wall can be divided into six segments according to the 17 AHA segment model [8].

At the anatomical level, the heart is a muscular organ acting as a mechanical pump. The cardiomyocytes are tightly coupled within the same laminar sheet, but sparsely coupled between adjacent laminar sheets. This structure makes the cardiac muscle an orthotropic tissue. Due to its anisotropy, the spatial variation of the fiber and laminar sheet orientations in the myocardium plays an important role in the realization of the cardiac function [9].

Study subjects

Clinical and dMRI imaging data were obtained in a group of 6 healthy subjects and 12 consecutive patients with a large [10] anterior AMI. The patients were treated according to current guidelines, including state-of-the-art interventional (primary PCI, pPCI, of the infarct-related artery, IRA) and pharmacologic therapy [11]. Care was taken to apply the existing measures to minimize myocardial tissue injury associated with ischemia and reperfusion, including, when applicable, thrombus aspiration [11–14]. In the AMI patients conventional MRI imaging was also performed to enable comparisons between DWI and conventional (late gadolinium-enhanced, LGE) images (for methods see ref. [10]). MRI was conducted several days after pPCI (first examination, hereinafter called E1) and 6 months later in the follow-up (second examination, hereinafter called E2). Research work and imaging were performed within the CIRCULATE Project of the National Centre for Research and Development (Poland) – STRATEGMED2. The study was approved by the Ethical Committee and all subjects provided written consent to participate.

In vivo cardiac DTI acquisition

Cardiac DTI was performed on a 3 T clinical MR scanner (Siemens MAGNETOM Skyra) equipped with an anterior cardiac 18-element matrix coil and a standard 45 mT/m gradient set with a slew rate of 200 T/m/s. All sequences were ECG-triggered. ECG trigger delay was acquired depending on the individual heart rate. Initially, the delay was set to be a half of an RR interval and then it was increased or decreased depending on the quality of a registered signal. Our pilot analysis showed that control of the signal quality in each slice was fundamen-

tal. DWIs were acquired during a single breath hold. DTI acquisitions were planned for the short axis view of the heart and 4 parallel slices were acquired along the long axis of the left ventricle.

Imaging was performed using a multi-shot SE-EPI readout (64 echoes per shot). Our pilot work on manipulating acquisition parameters to obtain highest-quality cardiac DWI led to the following protocol: TE = 64 (patient)/47 (control) ms, TR = 850 ms, field of view, FOV = 249 × 319 mm^2, voxel size: 0.83 × 0.83 × 8 (patient)/1.22 × 1.22 × 8 (control) mm^3, bandwidth, BW = 1630 Hz/Px, number of DW directions, N = 6, *b*-value, *b* = 350 s/mm^2, 1 scan. Modulation of these parameters was then used for imaging in study subjects.

Results and discussion

The present study enrolled 6 healthy volunteers and 12 consecutive patients with anterior AMI. Demographic and clinical data of study subjects are shown in Table I. Cardiac DWI imaging according to our algorithm was performed in all 18 cases, and consistent image patterns were obtained for (i) the healthy heart and (ii) the infarcted heart. Typical raw data are shown in Figure 1; average diffusivity values (± standard deviation lines) are displayed in Figure 2.

Our application of an SE-EPI sequence with cardiac gating allowed registration of a reasonable signal coming from the heart muscle (Figure 1). With our algorithm, this was achieved despite the reduced number of scans, lower *b*-value and increased resolution with lower attainable *TE* in comparison to the previous attempts [2, 10–17]. Considerably shorter *TE* in cardiac DTI can be indeed found in the literature, but for the stimulated-echo (STE) based sequences, which enable dMRI with the same *b*-value, but lower SNR [18]. However, due to lower SNR, STE is usually applied with multiple scans. This, for a moving object like the heart, can lead to erroneous averaging. *MD* and different tensor metrics can also be more accurately determined by using SE sequences [16]. We hypothesize, similarly to Mekkaoui *et al.* [2], that in the near future a major move from STE to SE-based imaging will occur in cardiac DTI. This move is anticipated to be facilitated by the increasing availability of clinical scanning at higher magnetic field gradients [2].

Our work indicates that the A1 and A2 segments may be highly discernible on DW images obtained according to our algorithm. This is particularly relevant for the myocardial infarction zone in these segments (note DWI signal hyperintensity in Figure 1 A, DWI 1-6, white arrows). No hyperintense spots were visible for the healthy control.

There were some important features in the DWI images, interesting for dMRI of AMI patients. Patient had an implanted stent (Figures 1 A, B, D, blue arrowhead on the left), which in DWI images is visible as a diffusion signal loss. Moreover, adjacent fatty accumulation (Figures 2, B, D blue arrowhead on the right) caused an effect similar to the infarction. Therefore, referential MRI (e.g. T_1, T_2) or additional clinical data are required for a proper interpretation of dMRI. Multi-shot SE-EPI with our algorithm enabled the application of a high resolution, which greatly helped to capture the details of the infarction areas – strong hyperintense spot, uniform across the myocardial wall. As shown by Mazur *et al.* [1], using the same algorithm for the patient shortly after the myocardial infarction incident it was also possible to distinguish a hypointense area reflecting microvascular obstruction between hyperintense strand-like areas associated with infarction [1]. This shows that with a carefully chosen SE-EPI DTI sequence protocol, details of the damaged zones can be almost as visible as in LGE images (Figures 1 C, D).

Table I. Clinical characteristics of healthy controls and study patients that provided initial clinical data from the AMI trial

Parameter	Healthy controls (*n* = 6)	Myocardial infarct (MI) patients (*n* = 12)
Age [years] median (range)	23.5 (19–28)	63 (43–74)
Gender (male/female) (percent of males)	3/3 (50%)	9/3 (75%)
BMI [kg/m^2] median (range)	21.26 (20.7–25.71)	27.41 (20.76–38.75)
Peak CK-MB [IU/l] median (range)	N/A	491 (135.6–607)
Time from MI to MRI [days] median (range)	N/A	7 (3–18)
Infarct vessel	N/A	LAD
Diabetes mellitus (DM) *n* (%)	N/A	3 (25)
Left ventricle ejection fraction (LVEF) – by echocardiography, median (range)	N/A	32% (23–41%)
LVEF by magnetic resonance imaging (MRI) median (range)	N/A	36% (19–42%)
Infarct size (IS) in MRI, median (range)	N/A	53% (39–76%)

LAD – left anterior descending artery.

Figure 1 B shows the method for distinguishing damaged myocardial zones. We propose to average all DWIs (from Figure 1 A), rescale all subjects to the same intensity range to enable inter-patient comparison and then increase the contrast by changing the display range. In this way, consecutive display shows more hyperintense spots, while the most severe damage appears first and the most benign last (Figure 2 B from top to bottom im-

ages). This is an important area for further research as DWI of the heart might depict areas with subtle damage that may be particularly amenable to myocardial reparation and regeneration using cell-based and other agents [10, 19]. In contrast, the post-infarction scar (classically viewed as "irreversible" injury that may be less amenable to cellular reparation in absence of simultaneous scaffold use [19, 20]) might be better distinguished using typi-
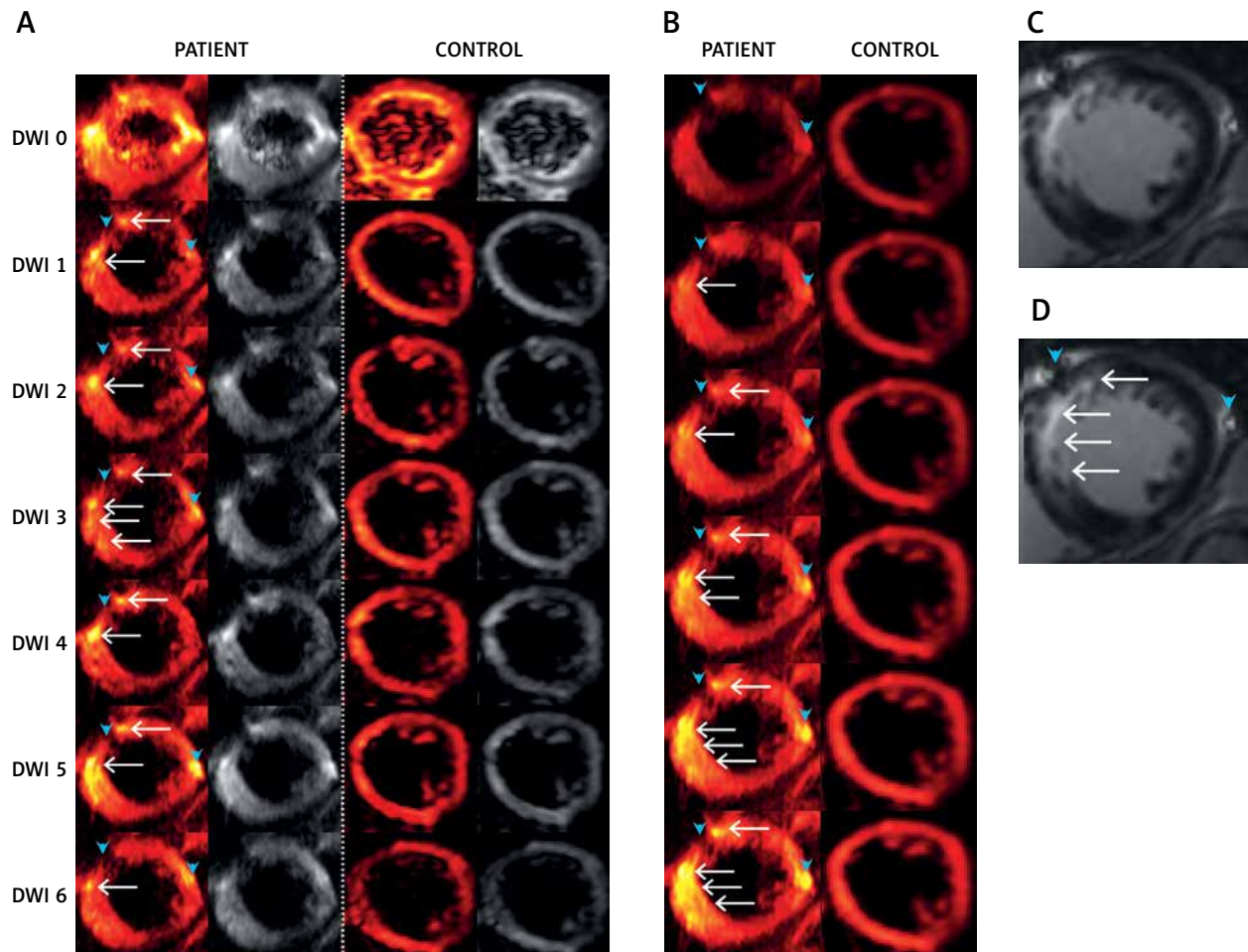

Figure 1. Typical examples of diffusion-weighted images of the human heart *in vivo* using the methodology we have developed. Images are from a patient (PATIENT) with acute anterior myocardial infarction (day 6 after pPCI) and from a healthy control (CONTROL). **A** – Raw multi-directional DWI images used for diffusion tensor calculation; **B** – use of an increased image contrast to enhance visualization of the hyperintense spots (infarct area according to classic gadolinium imaging). In (**A**) and (**B**) from top to bottom – diffusion-weighted images for b = 0 s×mm^{-2} (DWI 0) and six DWIs (DWI 1-6; from top to bottom) obtained for different non-collinear directions (hot color scale, left side, and gray scale, right side of each panel) (**A**). Images obtained using an increasing gradient of auto-contrasting (from top to bottom) (**B**). Typical T_1-weighted images with late gadolinium enhancement of the same patient heart (infarct areas indicated by white arrows; reference images). **C**, **D** – White arrows indicate infarct areas, blue arrowheads indicate vascular scaffold and fatty signal, while white arrowheads indicate microvascular obstruction zone. Note: (i) feasibility to obtain the human heart DWI images using the algorithm that we have developed, and (ii) increased DWI signal intensity in the infarcted areas, particularly visible on image contrast enhancement (**B**), allowing one to achieve improved visualization that is independent of the DWI direction and may be useful clinically, particularly as subtle damage areas are identified that are only in part amenable to conventional gadolinium contrast-based cardiac MRI imaging (see text for details)
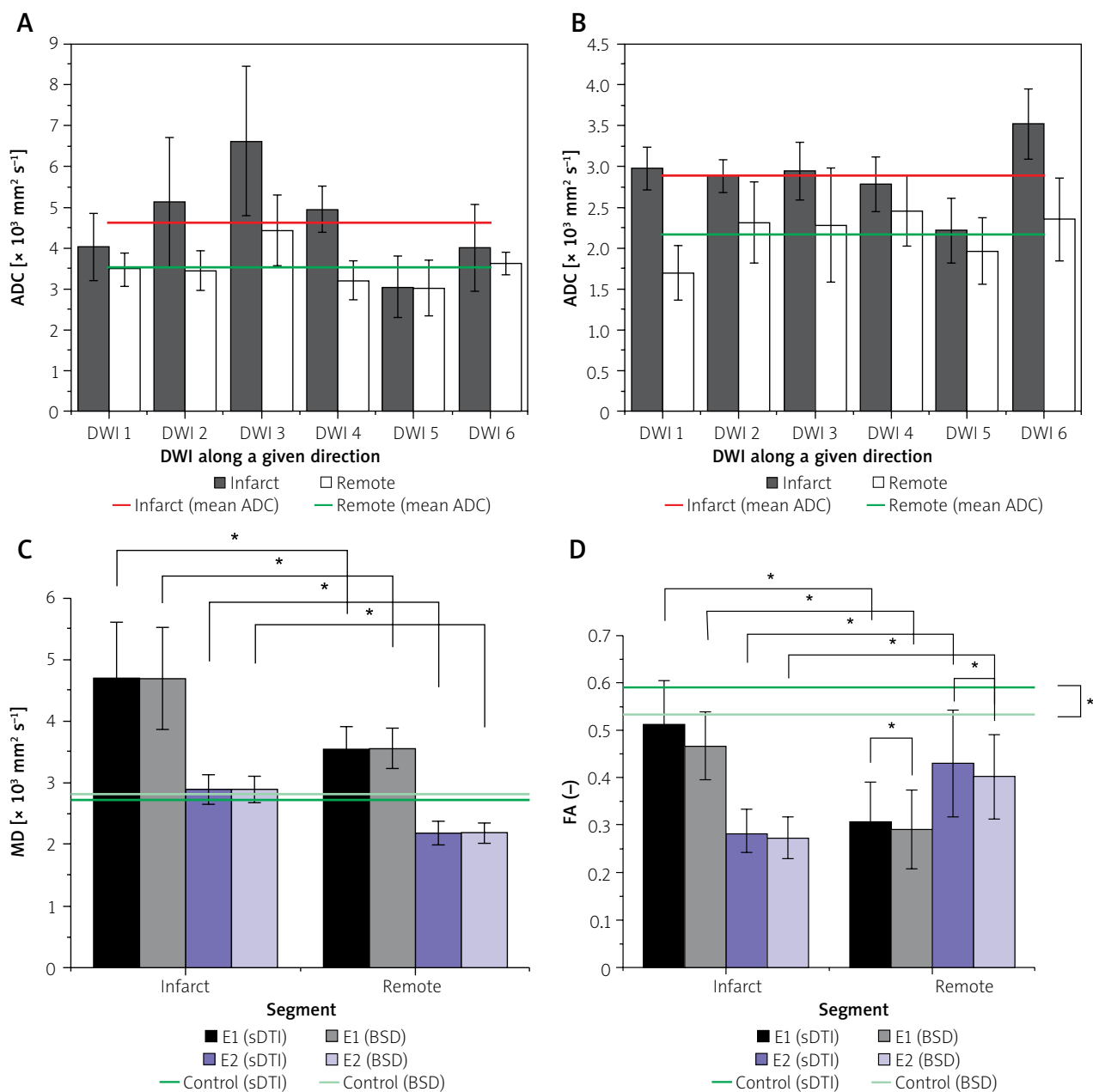
Figure 2. Average values (plotted with standard deviations) of the obtained DTI parameters: apparent diffusion coefficients (*ADC*s) for each of the non-collinear directions of DWI signal acquisition modes (DWI 1-6) according to our algorithm in infarct segment A2 and in remote tissue in E1 – 6 days after pPCI (**A**) and in the follow-up examination E2 (**B**). Mean diffusivity (*MD*) is shown in (**C**), whereas (**D**) shows fractional anisotropy (*FA*). In the plots statistically significant differences are designated (with 0.05 significance level)

cal contrast-enhanced MRI imaging (cf., Figure 1 B). Our findings are consistent with the concept that cardiac DWI might make it possible to reveal (and potentially quantify) less severely damaged regions of the heart and that this imaging modality might play an important role in monitoring the effect of therapies aimed at myocardial reparation and regeneration [4, 20, 21].

Quantitative dMRI was performed by determination of the apparent diffusion coefficient (*ADC*) along 6 differ-

ent directions and diffusion tensor parameters. *ADC*s for the patient obtained in E1 (6 days after pPCI) are overestimated for both infarcted and normal (or remote) tissue (Figure 2 A), and even exceed $D_0 = 3.04 \times 10^{-3}$ mm^2 s^{-1}, which is the value for free water at 37°C. Six months later in the follow-up examination (E2, Figure 2 B), *ADC*s are below D_0, but still slightly exceed the values of 0.73–2.4 $\times 10^{-3}$ mm^2 s^{-1} and 0.6–1.65 $\times 10^{-3}$ mm^2 s^{-1} reported for diseased and healthy/remote myocardium, respectively

[22–27]. Values as high as ~1.7–9 × 10^{-3} mm^2 s^{-1} are indeed encountered in the literature, but we would like to highlight again, after Stoeck *et al.* [28], that they result from motion-induced signal losses and cannot be connected with any physiological condition. Thus, we can recognize the influence of uncompensated motion on the *ADC*s from our study. Recent findings on the left ventricle motion dyssynchrony in infarct patients based on apical rocking suggest that dyssynchrony is the lowest and not statistically different from the healthy control for infarctions located in A1 and A2 segments [29], which is in accordance with patients in our study. This may explain lower overestimation than that pointed out by Stoeck *et al.* [28]. Slightly overestimated *ADC*s in E2 may indicate a more regular heart rate and breathing that enabled the diffusion encoding in the more quiescent cardiac phase unattainable shortly after AMI. Even though out of range, *ADC* can reflect the quality of dMRI by using multi-shot SE-EPI unrecognizable visually or motion extent despite the most quiescent cardiac phase chosen. The comparison between E1 and E2 results suggests that single heartbeat sequence design enabling free breathing is desirable for AMI patients. More reliable results in E2 indicate improved capacity for breath-holding and correspondingly overall health status.

Diffusion tensor was calculated from 7 DWIs obtained for all study subjects applying the standard (sDTI) and calibration (BSD) approach. Either sDTI or BSD delivered elevated mean diffusivity (*MD*, Figure 2 C) similarly to *ADC*s, while *MD* in E2 is again closer to the reported diffusivities for both infarct and remote areas. Even though motion can be recognized based on *ADC*s and *MD*, its influence can be assumed higher in remote than in the infarct area, where cardiomyocytes are affected and generate reduced force. Although higher overestimation is expected in the remote zone, the obtained diffusivities are still smaller than in the infarct area. Therefore, increased diffusivity in infarcted areas in comparison to remote tissues can also be expected in motion-compensated dMRI, similarly to the results presented by Moulin *et al.* [24] and Nguyen *et al.* [27].

Based on *ADC*s it can be seen that one direction where motion dominates cannot be recognized in E1's remote area and E2. Considering this and the fact that myocardial motion is complex in terms of type (strain, rotations, etc.) and direction, its approximately even influence on DWI 1-6 can be assumed. Then, fractional anisotropy (*FA*) should be close to the real values for E2 and remote in E1. The *FA* value obtained in E2 was *FA* = 0.282 ±0.052/0.272 ±0.044 (sDTI/BSD) for the infarct area, *FA* = 0.43 ±0.11/0.402 ±0.090 (sDTI/BSD) for remote tissues and *FA* = 0.59 ±0.15/0.53 ±0.13 (sDTI/BSD) for the control. These values are within the reported ranges: 0.26 for AMI [23], 0.36 for remote area and 0.54–0.55 for healthy control in diastole phase [26]. The elimination of systematic errors showed no influence on *MD*, but visibly improved *FA*.

Conclusions

The DWI image acquisition algorithm that we have developed enabled registration of adequate quality myocardial DWI images that showed differences between healthy subjects and AMI patients. The algorithm involves applying tailored SE-EPI sequences that take into consideration the subject's health status in relation to the breath-holding capability. This was achieved by our application of a small *b*-value, short *TE*, increased resolution and individually adjusted triggering. The differences between *MD* and *FA* obtained for the AMI patients' infarct vs. remote areas suggest that diffusion as a natural contrast can be a potential marker for subtle, early myocardial ischemic damage detection, similar to the role played by DWI imaging in basic research, clinical decision-making and evaluating the efficacy of novel therapies in cerebral ischemic injury [30]. Further progress in cardiac DWI imaging is anticipated to occur with triggering improvements and *TE* reduction to enable the standard SE-EPI sequence to be used in clinical practice.

Acknowledgments

Conflict of interest

The authors declare no conflict of interest.

References

1. Mazur W, Krzyżak AT, Hennel F. Diffusion-weighted imaging and diffusion tensor imaging of the heart in vivo: major developments. Adv Interv Cardiol 2022; 18: 350-9.
2. Mekkaoui C, Reese TG, Jackowski MP, et al. Diffusion MRI in the heart. NMR Biomed 2017; 30: e3426.
3. Borkowski K, Kłodowski K, Figiel H, et al. A theoretical validation of the B-matrix spatial distribution approach to diffusion tensor imaging. Magn Reson Imaging 2017; 36: 1-6.
4. Borkowski K, Krzyżak AT. Analysis and correction of errors in DTI-based tractography due to diffusion gradient inhomogeneity. J Magn Reson 2018; 296: 5-11.
5. Borkowski K, Krzyżak AT. Assessment of the systematic errors caused by diffusion gradient inhomogeneity in DTI-computer simulations. NMR Biomed 2019; 32: e4130.
6. Sosnovik DE, Mekkaoui C, Huang S, et al. Microstructural impact of ischemia and bone marrow-derived cell therapy revealed with diffusion tensor MRI Tractographyof the heart in vivo. Circulation 2015; 129: 1731-41.
7. Froeling M, Strijkers GJ, Luijten PR. Diffusion tensor MRI of the heart – in vivo imaging of myocardial fiber architecture. Mol Imaging 2014; 7: 926.

8. Cerqueira MD, Weissman NJ, Dilsizian V, et al. Standardized myocardial segmentation and nomenclature for tomographic imaging of the heart. A statement for healthcare professionals from the Cardiac Imaging Committee of the Council on Clinical Cardiology of the American Heart Association. Circulation 2002; 105: 539-42.

9. Nielles-Vallespin S, Mekkaoui C, Gatehouse P, et al. In vivo diffusion tensor MRI of the human heart: Reproducibility of breath-hold and navigator-based approaches. Magn Reson Med 2013; 70: 454-65.

10. Musiałek P, Tekieli L, Kostkiewicz M, et al. Infarct size determines myocardial uptake of CD34+ cells in the peri-infarct zone: results from a study of (99m)Tc-extametazime-labeled cell visualization integrated with cardiac magnetic resonance infarct imaging. Circ Cardiovasc Imaging 2013; 6: 320-8.

11. Ibanez B, James S, Agewall S, et al. 2017 ESC Guidelines for the management of acute myocardial infarction in patients presenting with ST-segment elevationThe Task Force for the management of acute myocardial infarction in patients presenting with ST-segment elevation of the European Society of Cardiology (ESC). Eur Heart J 2018; 39: 119-77.

12. Zalewski J, Zmudka K, Musiałek P, et al. Detection of microvascular injury by evaluating epicardial blood flow in early reperfusion following primary angioplasty. Int J Cardiol 2004; 96: 389-96.

13. Musiałek P. Coronary thrombus management. In: Treatment Strategies – Interventional Cardiology. Eeckhout E, Evangelista A, Holmes D, et al. (eds.). Cambridge Research Centre UK 2012; 97-106.

14. Musiałek P. A TASTE-less endpoint of 30-day mortality (and some other issues with TASTE) in evaluating the effectiveness of thrombus aspiration in STEMI: not the "evidence" to change the current practice of routine consideration of manual thrombus extraction. Kardiol Pol 2014; 72: 479-87.

15. Nielles-vallespin S, Mekkaoui C, Gatehouse P, et al. In vivo diffusion tensor MRI of the human heart: reproducibility of breath-hold and navigator-based approaches. Magn Reson Med 2013; 465: 454-65.

16. Deuster C Von, Stoeck CT, Genet M, et al. Spin echo versus stimulated echo diffusion tensor imaging of the in vivo human heart. Magn Reson Med 2016; 872: 862-72.

17. Scott AD, Nielles-vallespin S, Ferreira PF, et al. An in-vivo comparison of stimulated-echo and motion compensated spin-echo sequences for 3 T diffusion tensor cardiovascular magnetic resonance at multiple cardiac phases. J Cardiovasc Magn Reson 2018; 20: 1.

18. Volovyk O, Tal A. Application of phase rotation to STRESS localization scheme at 3 T. Magn Reson Med 2017; 79: 2481-90.

19. Karama J, Muscari C, Montero-Menei C. Combining adult stem cells and polymeric devices for tissue engineering in infarcted myocardium. Biomaterials 2012; 33: 5683-95.

20. Musiałek P. The Krakow Myocardial Regeneration Team impact on the global progress in the field of pre-clinical and clinical progenitor cell therapy: inventions and innovations in 2002-2015. In: Innovative Technologies in Biomedicine. Figiel H, Undas A, Gajos G (eds.). The Cracovian Association for Heart and Lung Health PULMO-COR 2015; 115-38.

21. Tomanek B. Advanced imaging and image-guided technologies. Innov Technol Biomed 2015; 19-21.

22. Aliotta E, Moulin K, Zhang Z, et al. Simultaneous measurement of T2 and apparent diffusion coefficient (T2+ADC) in the heart with motion-compensated spin echo diffusion-weighted imaging. Magn Reson Med 2018; 79: 654-62.

23. Wu MT, Tseng WYI, Su MYM, et al. Diffusion tensor magnetic resonance imaging mapping the fiber architecture remodeling in human myocardium after infarction: correlation with viability and wall motion. Circulation 2006; 114: 1036-45.

24. Moulin K, Viallon M, Romero W, et al. MRI of reperfused acute myocardial infarction edema: ADC quantification versus T1 and T2 mapping. Radiology 2020; 295: 542-9.

25. Nguyen C, Lu M, Fan Z, et al. Contrast-free detection of myocardial fibrosis in hypertrophic cardiomyopathy patients with diffusion-weighted cardiovascular magnetic resonance. J Cardiovasc Magn Reson 2015; 17: 107.

26. Tunnicliffe EM, Scott AD, Ferreira P, et al. Intercentre reproducibility of cardiac apparent diffusion coefficient and fractional anisotropy in healthy volunteers. J Cardiovasc Magn Reson 2014; 16: 31.

27. Nguyen C, Fan Z, Xie Y, et al. In vivo contrast free chronic myocardial infarction characterization using diffusion-weighted cardiovascular magnetic resonance. J Cardiovasc Magn Reson 2014; 16: 68.

28. Stoeck CT, Scott AD, Ferreira PF, et al. Motion-induced signal loss in in vivo cardiac diffusion-weighted imaging. J Magn Reson Imaging 2020; 51: 319-20.

29. Steelant B, Stankovic I, Roijakkers I, et al. The Impact of infarct location and extent on LV motion patterns: implications for dyssynchrony assessment. JACC Cardiovasc Imaging 2016; 9: 655-64.

30. Traenka C, Engelter S, Brown M, et al. Silent brain infarcts on diffusion-weighted imaging after carotid revascularisation: a surrogate outcome measure for procedural stroke? A systematic review and meta-analysis. Eur Stroke J 2019; 4: 127-43.